TÜBİTAK

Turkish Journal of Chemistry

http://journals.tubitak.gov.tr/chem/

Research Article

Turk J Chem
(2018) 42: 274 – 290

doi:10.3906/kim-1705-59

Spectroscopic and thermodynamic approach to the interaction of nonperipherally substituted cationic phthalocyanines with calf thymus (CT)-DNA

Sevgican TUNCER, İbrahim ÖZÇEŞMECİ, Behice Şebnem SESALAN, Ayfer KALKAN BURAT*

Department of Chemistry, Faculty of Science and Letters, İstanbul Technical University, İstanbul, Turkey

Received: 30.05.2017 • **Accepted/Published Online:** 25.09.2017 • **Final Version:** 27.04.2018

Abstract: Novel, nonperipherally tetrasubstituted cationic metal-free and metallophthalocyanines (Zn, In) were synthesized in the present study. The binding constants, the disappearance of quenching effect of all cationic phthalocyanines on the fluorescence intensity of SYBR Green–disodium salt of deoxyribonucleic acid (DNA) from calf thymus complex, and the changes in T_m of double helix DNA with thermal denaturation profile were investigated by UV-Vis and fluorescence spectrophotometric methods. To investigate the spontaneity of the reactions between DNA and novel quaternized phthalocyanines in buffer, thermodynamic parameters were employed.

Key words: Calf thymus (CT)-DNA, morpholine, quaternized phthalocyanines, Gibbs, entropy

1. Introduction

The interaction of metal complexes with deoxyribonucleic acid (DNA) has been investigated for a long time and the scope of synthesis of new reagents was to be beneficial for biotechnology and medicine.[1] Among such reagents, cationic porphyrins and their related analogues are known to bind to DNA.[2] Three binding modes with DNA were suggested: (a) intercalation; macrocycles intercalate into the bases of nucleic acids (like a step in the DNA ladder), (b) groove binding involves van der Waals interaction with the bases in the major groove or the shallow minor groove of the DNA helix, and (c) outside electrostatic binding with aggregated porphyrins stacked along the DNA helix.[3,4]

Phthalocyanines (Pcs), derivatives of porphyrins, are highly conjugated macrocycles with interesting properties that allow them to be beneficial for many research areas, such as dyes, catalysts, semiconductors, electrochromic devices, liquid crystal displays, nonlinear optical, and photovoltaic cells and make them attractive reagents for nucleic acid modification.[5–10] The therapeutic applications of Pcs require them to be soluble in buffer. To circumvent this restriction, Pcs are substituted with different units that enable them to dissolve in water or buffer.[11–14] Even though most of the water-soluble Pcs dimerize and aggregate in aqueous solution, there are nonaggregated Pcs in the literature.[15,16] The efficiency of aggregation strongly affects the photophysical and physicochemical properties of Pcs.[17,18] It was reported that nonperipheral substituted Pcs decreased the aggregation.[15,16,19–21]

Although the interaction of peripherally tetrasubstituted cationic Pcs with single- and double-stranded DNA has attracted a great deal of interest, nonperipherally substituted cationic Pcs are less studied.[22,23] The

*Correspondence: kalkanayf@itu.edu.tr

affinity of cationic porphyrins for DNA and RNA was reported three decades ago and it has stimulated many further studies.[3,24]

The need for new drugs for cancer has forced chemistry to use the main classes of chemical compounds with new methods as alternative to old techniques. Recently, Pcs and their cationic derivatives have been of interest for research in medicine and biology.[25–27] In addition, morpholine and its derivatives display a wide spectrum of medicinal activities such as anticancer and antioxidant.[28,29] Morpholine derivatives are in development as pharmaceutical therapeutics targeting pathogenic organisms such as bacteria and viruses.[30–32] The presence of morpholine groups in the structure of water-soluble Pcs can increase their bioavailability and anticancer effects. It will be interesting to investigate the biological properties of new water-soluble Pcs appended with morpholinoethoxy groups. Hence, recently we have focused on the synthesis and investigation of nonperipherally substituted cationic Pcs. Our previous studies reported the biological efficacy of novel peripherally substituted quaternized Pcs to assess their potential application in PDT.[33–37] From this point of view, the aim of the present study was to synthesize novel nonperipherally tetrasubstituted quaternized metal-free (**1Q**), zinc (**2Q**), and indium (**3Q**) Pcs appending 2-morpholinoethoxy groups that have potential use in biology. UV-Vis and fluorescence titration experiments were done to determine the binding mode of quaternized Pcs to CT-DNA. The self-assembly properties of **1Q**–**3Q** in buffer solution (pH 7) were comparatively investigated. Furthermore, the effect of **1Q**, **2Q**, and **3Q** on the fluorescence quenching of SYBR Green–DNA complex was examined. In addition, for a deeper look into the binding process, the energetics were examined with the employment of thermodynamic parameters such as enthalpy, entropy, Gibbs free energy, and K_{eq} equilibrium constant.

2. Results and discussion

2.1. Synthesis and characterization

The synthetic pathway for the cationic Pcs (**1Q**–**3Q**) is represented in Scheme 1. The synthesis of water-soluble metal-free (**1Q**), zinc (**2Q**), and indium (**3Q**) Pcs was achieved by the reaction of corresponding Pcs (**1**–**3**) with excess methyl iodide in $CHCl_3$ at reflux temperature for 4 h. The desired Pcs (**1Q**–**3Q**) were washed successively with hot solvents like ethyl acetate, THF, ethanol, chloroform, diethyl ether, and n-hexane. Compounds **1Q**–**3Q** were characterized by spectroscopic methods (^{1}H NMR, FTIR, and UV-Vis spectra). The data are consistent with the assigned structures. The compounds (**1Q**–**3Q**) prepared in this study are soluble in DMSO, DMF, and water as expected.

The IR spectra of the Pcs **1Q**–**3Q** are very similar to each other. Aromatic CH, aliphatic CH, and C–O–C vibrations were observed at around 3018–3007, 2947–2869, and 1235–1217 cm^{-1}, respectively. The metal-free Pc (**1Q**) showed an additional absorption band at 3283 cm^{-1} assigned to the NH stretching vibrations.

In the ^{1}H NMR spectrum of metal-free Pc (**1Q**) in DMSO-d_6 the aromatic protons resonated between 9.22 and 8.04 ppm (Figure S1). The OCH_2 and NCH_2 protons were observed between 5.45 and 3.73 ppm. The inner core protons of free-base Pc (**1Q**) and the N^+–CH_3 protons were monitored at –0.13 and 3.67 ppm, respectively. In the ^{1}H NMR spectra of zinc (**2Q**) and indium (**3Q**) Pcs in DMSO-d_6 the aromatic protons of the Pc core resonated between 9.19 and 7.97 ppm for **2Q** and for **3Q** between 9.19 and 8.00 ppm, integrating for 12 protons for each complex (Figures S2 and S3). The OCH_2 and NCH_2 protons of tetracationic Pcs (**2Q**, **3Q**) were monitored between 5.50 and 3.56 ppm. One additional signal for N^+–CH_3 protons was observed as a singlet at 3.70 ppm for **2Q** and 3.68 ppm for **3Q**, respectively.

UV-Vis spectra of the quaternized metal-free and metallophthalocyanines exhibited Q bands at 697/724

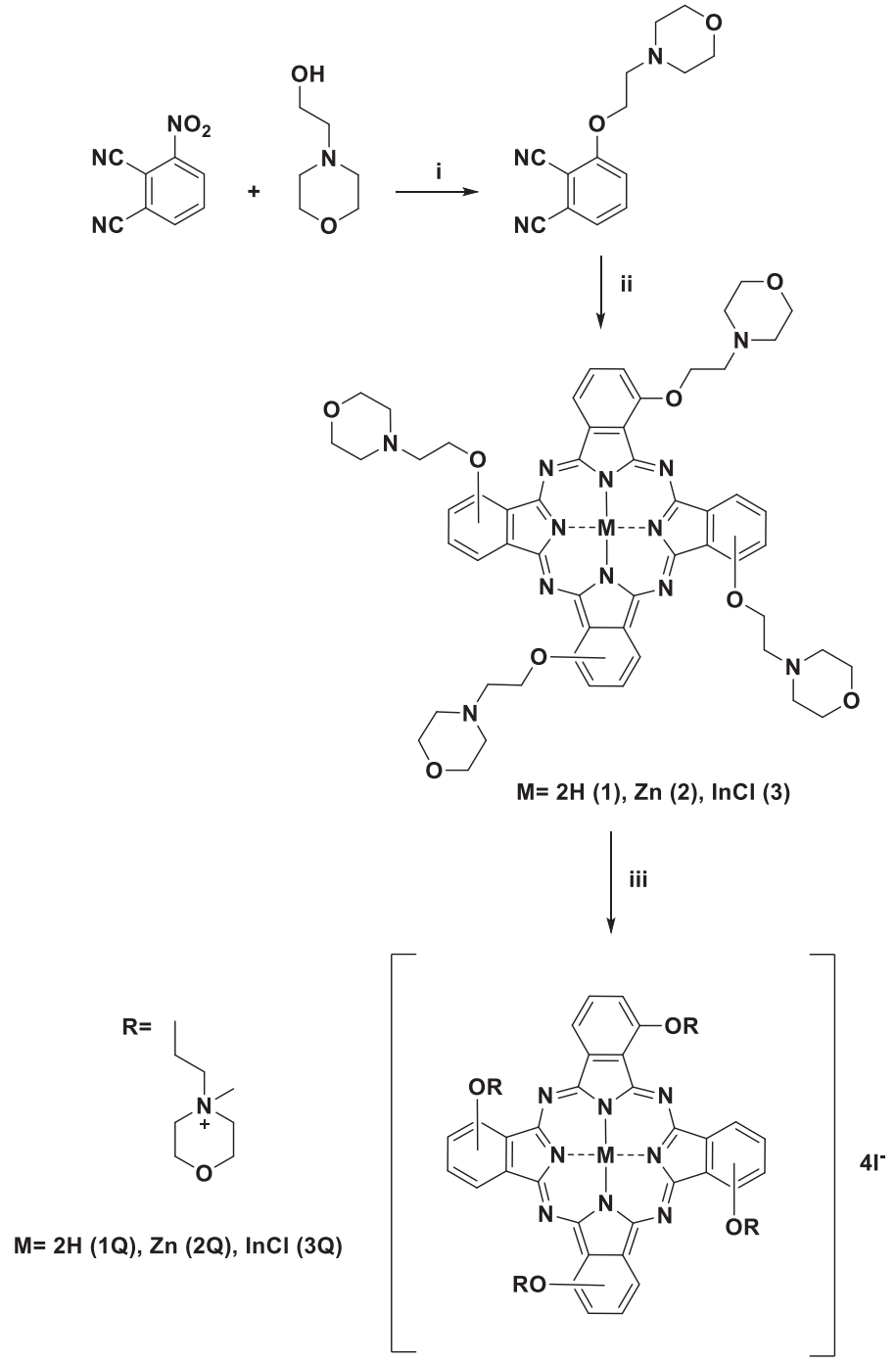

Scheme. The synthesis of quaternized phthalocyanines (**1Q**–**3Q**) starting from the corresponding phthalonitrile. (i) DMSO, K_2CO_3, room temperature, 72 h. (ii) 1-pentanol, DBU, metal salts (without metal salt for compound **1**), 145 °C, 24 h. (iii) $CHCl_3$, excess CH_3I, at dark, reflux temperature, 4 h.

nm for **1Q**, 698 nm for **2Q**, and 717 nm for **3Q** (Figure 1a) in DMF. The B band region was monitored around 318–325 nm. The electronic absorption spectra of these compounds in DMF are typical for nonaggregated Pcs, exhibiting intense and sharp Q-bands. The Q bands of the nonperipheral tetrasubstituted complexes (**1Q**–**3Q**)

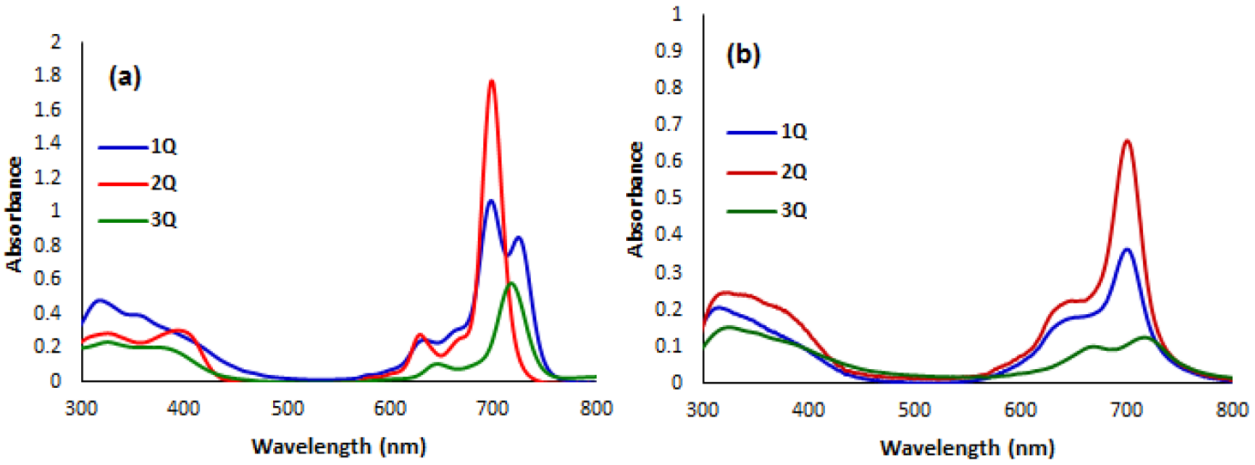

Figure 1. UV-Vis absorption spectra of quaternized metal-free (**1Q**), zinc (**2Q**), and indium (**3Q**) phthalocyanines (a) in DMF (1×10^{-5} M) (b) in water (1×10^{-5} M).

red-shifted by 20–25 nm, when compared to the corresponding Pcss carrying morpholine moieties at axial or peripheral positions, suggesting the effect of substituents at the α-position on the Q-band position is essentially additive.[38,39] This red-shift phenomenon is consistent with previous reports for nonperipherally substituted Pcs, and supports the explanation that substitution at the α-position can lead to reduction of the HOMO-LUMO gap.[40–42] However, the electronic spectra of the compounds (**1Q**–**3Q**) in water showed some differences from those in DMF. The broadening of the Q bands and the decrease in the intensity of the Q bands corresponded to the presence of aggregated species in aqueous media compared to the electronic spectra in DMF. The B and Q bands of the compounds (**1Q**–**3Q**) in water were observed around 319–324 nm and 700–717 nm, respectively (Figure 1b) (Table S1). The absorption spectra of **1Q**–**3Q** were also recorded in both Triton X-100 and pyridine. As shown in Figure 2, addition of Triton X-100 (5% and 10%) to the aqueous solution of **1Q**–**3Q** did not cause an important increase in intensity of Q bands. However, addition of pyridine caused a significant increase in the intensity of Q bands (Figure S4). To test the aggregation of the complexes (**1Q**–**3Q**) dilution studies in water were done for concentrations ranging from 5.00×10^{-5} to 3.125×10^{-6} M (Figure S5). As the concentration was increased, the intensity of absorption of the broad Q band also increased.

2.2. Evaluation of UV-Vis spectra of quaternized Pcs (1Q–3Q) with CT-DNA

UV-Vis spectroscopy is an important technique for investigating the binding mode of compounds with CT-DNA.[43] In the UV-Vis region, the spectroscopic change with the interaction of compounds with DNA indicates the binding mode. Generally, metal compounds can bind to DNA via covalent or noncovalent binding such as intercalation, major and minor groove binding (binding of the compounds outside of DNA), and electrostatic interactions. DNA intercalating agents cause large shifts at wavelengths in the UV-Vis spectrum. However, stacking causes small changes in absorbances or wavelengths.[44]

The absorption spectra of quaternized metal-free (**1Q**), zinc (**2Q**), and indium (**3Q**) Pcs in the absence and presence of CT-DNA were recorded ranging from 300 to 800 nm and can be observed in Figure 3. When a stable DNA–Pc complex formed, maximal absorbances of **1Q**–**3Q** decreased as a result of interaction with DNA. The last lines in Figure 3 recorded on top of each other mean that after addition of 180 μL of DNA to

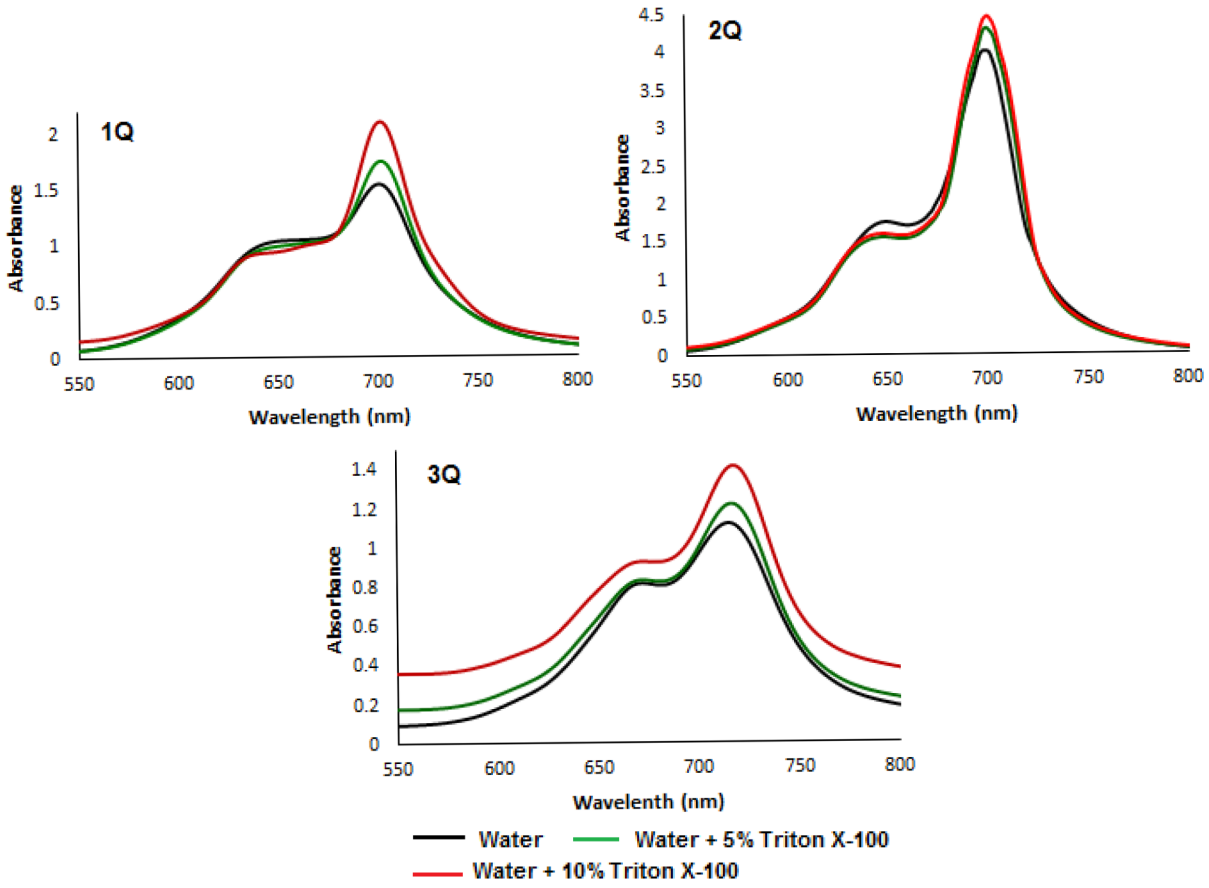

Figure 2. UV-Vis absorption spectra of quaternized metal-free (**1Q**), zinc (**2Q**), and indium (**3Q**) phthalocyanines in water (5×10^{-5} M) and water containing Triton X-100.

metal-free (**1Q**), zinc (**2Q**), and indium (**3Q**) Pcs the Q band absorbance remained constant. They showed the end of titration, which means the maximum interaction between Pcs and DNA occurred. The hypochromism suggested a close positioning of cationic Pcs (**1Q**–**3Q**) to the DNA helix due to strong electrostatic interactions between the positive charge morpholinoethoxy groups and phosphate backbone of DNA.

Proteins with zinc finger motif have high affinity to DNA and bind in the major groove.[45] It is known that the interaction of purines and/or pyrimidines with chelating compounds destabilizes the nature of DNA.[46,47] The appearance of absorptions belonging to monomeric **2Q** displayed the interaction of zinc with bases in DNA. As shown in Figure 3, DNA bases (especially with basic N7 donors in guanines) could coordinate to zinc. Moreover, oxygens in phosphates stabilize monomeric **2Q** via coordinating to zinc. However, more experiments should be employed to determinate that **2Q** is a major groove binder. Thus, according to $K_{b\mathbf{2Q}}$, it binds DNA nonspecifically (Table 1).

In the case of **3Q**, taking into consideration intermolecular forces set by hydrogen bonds formed by chlorine and hydrogens present in DNA bases, the presence of monomeric species observed at 717 nm could be attributed to indium–DNA interactions referring to metal–DNA coordination (Figure 3). Compared with quaternized metal-free (**1Q**) and zinc Pcs (**2Q**), a further interaction due to chlorine was the main reason for a lower K_b value for **3Q**.

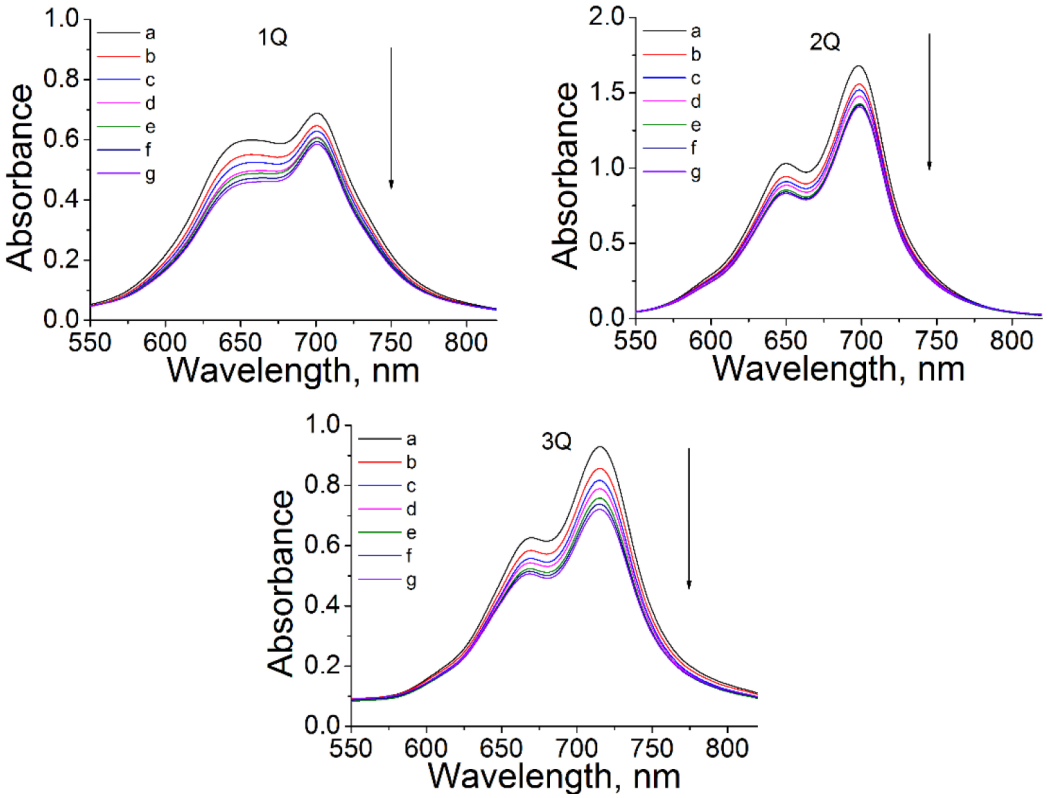

Figure 3. Spectroscopic changes in the UV-Vis absorption spectrum of quaternized metal-free (**1Q**), zinc (**2Q**), and indium (**3Q**) phthalocyanines (2.5×10^{-6} M) in buffer solution upon addition of DNA (a = 0 M; b = 4.95×10^{-7} M; c = 9.80×10^{-7} M; d = 1.46×10^{-6} M; e = 1.92×10^{-6} M; f = 2.38×10^{-6} M; g = 2.83×10^{-6} M).

Although nonperipheral substitution rather than peripheral decreased the aggregation, metal-free Pc rings aggregated quite a lot.[38–40,48] In zinc and indium complexes, aggregation was lower and more monomeric forms were the prevailing species in buffer. The binding constants of **1Q**, **2Q**, and **3Q** were determined as $6.67 \pm (0.1) \times 10^5$ M^{-1}, $6.00 \pm (0.1) \times 10^5$ M^{-1}, and $3.50 \pm (0.1) \times 10^5$ M^{-1}, respectively (Table 1). According to the literature, the K_b values of anticancer agents such as idarubicin and doxorubicin ranged between 10^5 and 10^6 M^{-1}.[49,50] Such anticancer agents exhibited strong DNA binding affinity, but they have major side effects. However, Pcs do not harm normal tissue and positively charged Pcs show the most efficient interactions with DNA.[22,33,51] The results exhibited that **1Q**–**3Q** were able to bind CT-DNA with stronger binding affinity, and these K_b values proved that, with the addition of DNA, stable cationic Pc–DNA complexes formed via electrostatic attractions.[22,33,51]

Table 1. K_b values of **1Q**–**3Q** with standard deviations (± STD).

	K_b ($\times 10^5$)(L × mol^{-1})
1Q	6.67 ± 0.1
2Q	6.00 ± 0.1
3Q	3.50 ± 0.1

2.3. The evaluation of fluorescence spectra of quaternized Pcs (1Q–3Q) with CT-DNA

In order to calculate the binding constant of Pc to DNA, generally either absorbance or fluorescence titration is utilized. In our experiments, fluorescence titration was used to prove the binding mode. An important feature of fluorescence is that there is a rather direct connection between the spectroscopic observations and molecular features of the sample. Thus, it is a convenient way to visualize how the spectroscopic properties of **1Q**, **2Q**, and **3Q** complexes formed with DNA are affected by the polar aqueous environment.

The enhanced emission of cationic morpholinoethoxy units attached to hydrophobic Pc core might be the result of cumulative effects of electrostatic binding and strong hydrophobic association between the Pc core and hydrophobic interior of DNA.[52] In the fluorescence spectra of **1Q**, **2Q**, and **3Q** (Figure 4), a hydrophobic interaction results from the close positioning of Pc core to DNA helix due to the electrostatic attraction between cationic morpholinoethoxy groups and negative phosphates. Due to the addition of DNA, ionic parts of cationic Pcs form an outer shell in contact with water, while nonpolar Pc cores are sequestered in the interior to have minimum contact with water, which quenches fluorescence. As the water molecules were removed around Pcs, the intensities of emissions increased.

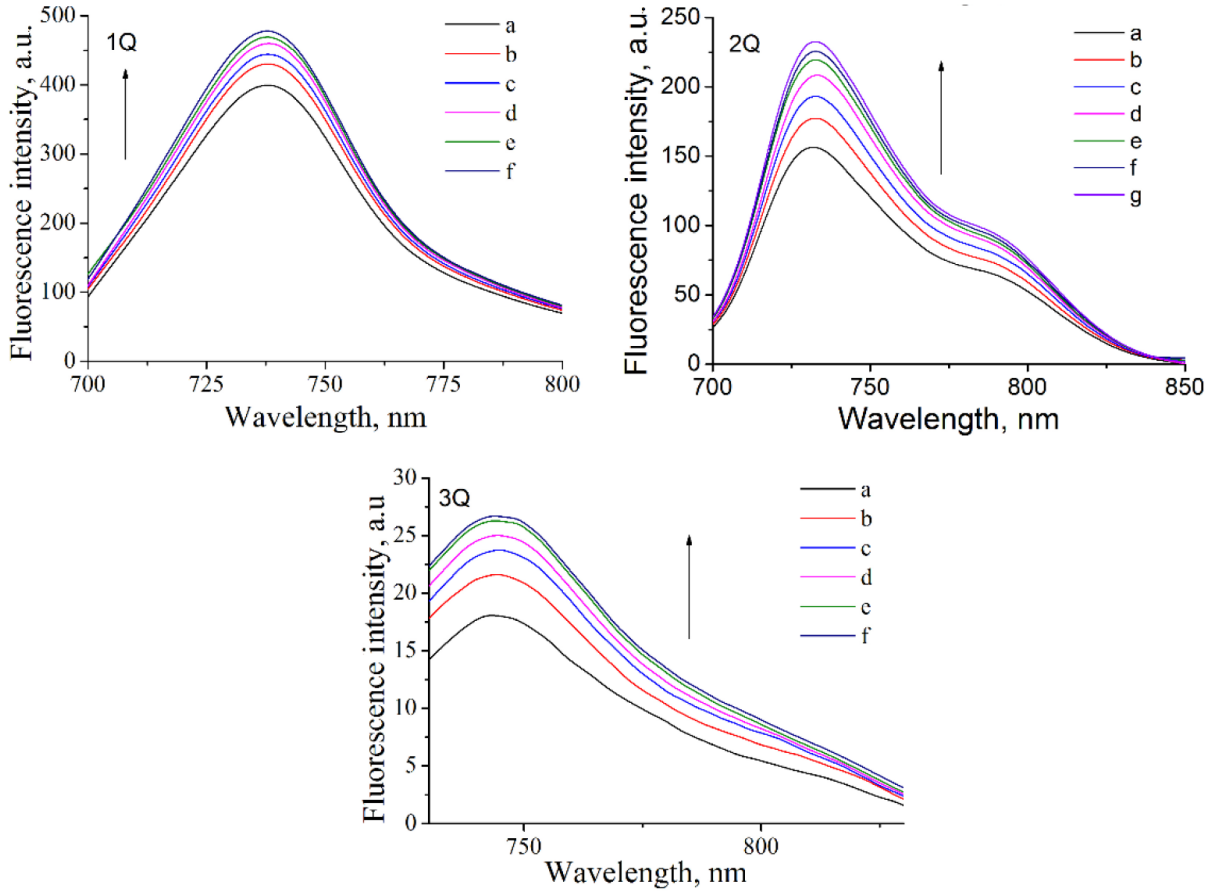

Figure 4. Spectroscopic changes in fluorescence emission spectrum of quaternized metal-free (**1Q**), zinc (**2Q**), and indium (**3Q**) phthalocyanines (2.5×10^{-6} M) in buffer solution upon addition of DNA (a = 0 M; b = 4.95×10^{-7} M; c = 9.80×10^{-7} M; d = 1.46×10^{-6} M; e = 1.92×10^{-6} M; f = 2.38×10^{-6} M; g = 2.83×10^{-6} M).

2.4. The effect of quaternized Pcs (1Q–3Q) on the fluorescence of SYBR–DNA complex

SYBR Green (SYBR) is a known DNA stain used in biological applications and greatly enhanced fluorescence at 527 nm is observed when bound to DNA.[53] Therefore, a competition of binding assay between SYBR and quaternized Pcs could determine the mode of interaction with DNA. Due to the electrostatic attractions between negative polymer DNA and cationic Pcs (**1Q**–**3Q**), stable Pc-DNA complexes were formed (Figures 5a–5c). Electrostatic repulsions were reduced in DNA and a more compact structure was formed (Figures 5a–5c). The contribution of cationic Pcs (**1Q**–**3Q**) to DNA–SYBR complex provided a more neutralized, rigid structure, causing an increase in emission. Figures 5a–5d proved that when rigidity arose in Pc–DNA complexes due to either electrostatic or hydrophobic interactions, the constriction to free rotational movements resulted in a considerable increase in emission. Figures 4 and 5a–5d were evidence for Pc–DNA complexes.

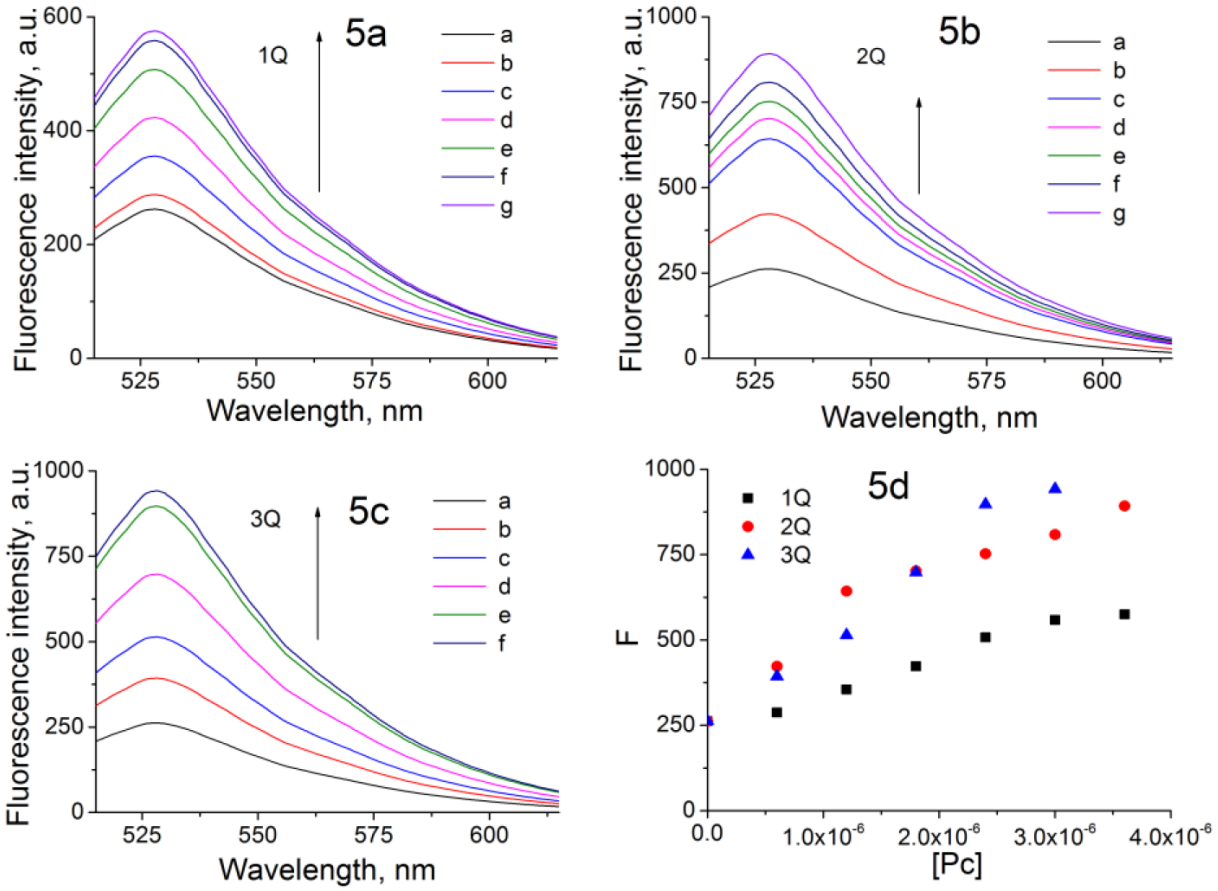

Figure 5. Spectroscopic changes in fluorescence emission spectrum of SYBR–DNA in buffer solution upon addition of quaternized metal-free (**1Q**) (5a), zinc (**2Q**) (5b), and indium (**3Q**) (5c) phthalocyanines (a = 0 M; b = 5.86 × 10^{-7} M; c = 1.15 × 10^{-6} M; d = 1.68 × 10^{-6} M; e = 2.19 × 10^{-6} M; f = 2.68 × 10^{-6} M; g = 3.15 × 10^{-6} M). The plot for F versus [Pc] (5d).

2.5. The evaluation of thermal denaturation profile of DNA

DNA melting profile is very informative about the stability of the helix. The thermal melting temperature (T_m) of DNA is defined as the temperature at which half of the DNA strands are in single-stranded (ssDNA)

state.[54] Thermal denaturation experiments can be employed to estimate the binding mode of DNA compounds as intercalative or electrostatic modes. In our experiments, the influence of cationic Pcs (**1Q**–**3Q**) on the stability of DNA duplex and strand dissociation was examined by thermal denaturation profile and is shown in Figure 6.

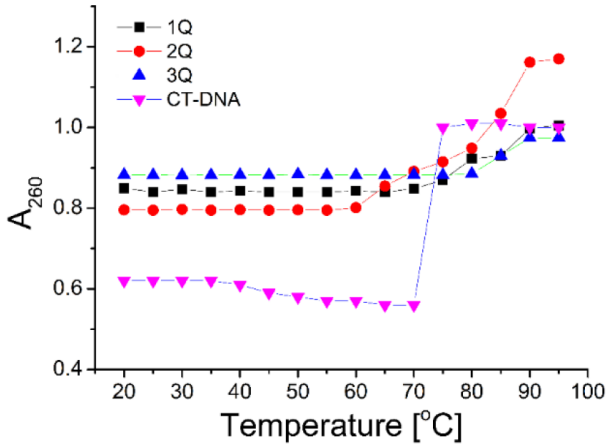

Figure 6. Thermal denaturation profiles of CT-DNA in the presence of quaternized metal-free (**1Q**), zinc (**2Q**), and indium (**3Q**) phthalocyanines.

Under the same set of conditions, in the presence of cationic Pcs, T_m values with standard deviations for **1Q**, **2Q**, and **3Q** were calculated as 72.5 ± 0.102 °C, 73.1 ± 0.88 °C, and 82.3 ± 0.112 °C, respectively. The T_m of DNA in the absence of any Pc was 70 ± 1 °C. The denaturation temperature (T_m) was taken as the mid-point of the hyperchromic transition. The melting temperature of DNA (T_m) in the presence of a binding molecule or metal can also be used to interpret different binding modes.[35] It is reported that a classical intercalation gives rise to higher T_m values than either groove binding or outside stacking.[35] The higher deviation in the T_m value of **3Q** indicated that hydrogen bonds between DNA and chlorine stabilized DNA more than metal-free (**1Q**) and zinc (**2Q**) Pcs.

Zinc–DNA coordination might destabilize the double strand nature of DNA, resulting in the dissolution of strands. Due to a possible zinc finger role of **2Q**, a stronger coordination with N/O donors in DNA destabilized DNA nature and resulted in the dissociation of the double strand DNA helix. Through both electrostatic and hydrophobic attractions, the closer positioning of planar Pc rings of **1Q**, **2Q**, and **3Q** to DNA might provide groove binding. However, more experiments are necessary to give details of the mechanism.

2.6. The evaluation of thermodynamics

Binding studies were carried out at 20, 30, 40, 50, and 60 °C. At these temperatures, DNA does not undergo any structural degradation. Three thermodynamic parameters, i.e. standard Gibbs free energy, ΔG°; the standard molar enthalpy, ΔH°; and the standard molar entropy, ΔS, were used to examine the spontaneity of reactions that take place between quaternized Pcs (**1Q**–**3Q**) and DNA. The Van't Hoff plots are shown in Figure 7 and ΔG°, ΔH°, and ΔS° energies with their deviations are given in Table 2.

The hydrophobic effect is the exclusion of water by hydrophobic groups. This appears to depend on the increase in entropy of solvent water molecules that are released from an ordered arrangement around the hydrophobic group. The change in enthalpy is insignificant in determining the spontaneity of the reaction

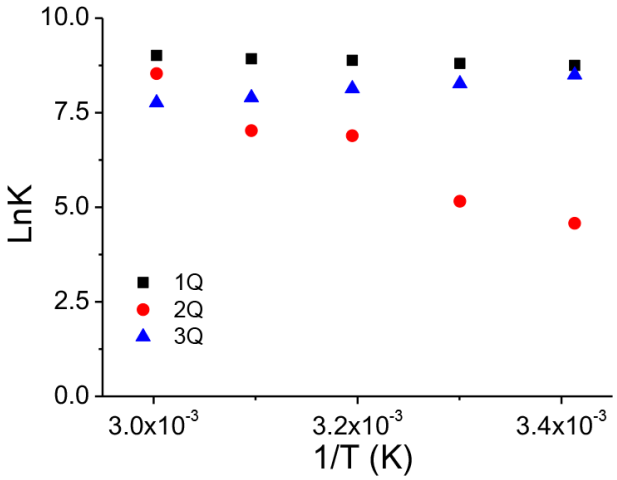

Figure 7. Van't Hoff plots of CT-DNA binding of quaternized metal-free (**1Q**), zinc (**2Q**), and indium (**3Q**) phthalocyanines.

Table 2. Calculated thermodynamic parameters for binding of **1Q**–**3Q** to CT-DNA.

T (K)	(LnK ±ΔK)	ΔG^o (kJ mol^{-1})	ΔH° (kJ mol^{-1})	$T\Delta S^\circ$ (kJ mol^{-1} K^{-1})
H_2Pc (**1Q**)				
293.15	8.75 ± 0.05	–21.29 ± 0.1	5.28 ± 0.1	26.57 ± 0.30
303.15	8.80 ± 0.05	–22.20 ± 0.1	5.28 ± 0.1	27.48 ± 0.30
313.15	8.88 ± 0.05	–23.11 ± 0.1	5.28 ± 0.1	28.39 ± 0.30
323.15	8.92 ± 0.05	–24.01 ± 0.1	5.28 ± 0.1	29.29 ± 0.30
333.15	9.01 ± 0.05	–24.92 ± 0.1	5.28 ± 0.1	30.20 ± 0.30
ZnPc (**2Q**)				
293.15	4.57 ± 0.05	–11.36 ± 0.1	67.98 ± 0.1	79.34 ± 0.30
303.15	5.16 ± 0.05	–14.06 ± 0.1	67.98 ± 0.1	82.04 ± 0.30
313.15	6.89 ± 0.05	–16.77 ± 0.1	67.98 ± 0.1	84.75 ± 0.30
323.15	7.03 ± 0.05	–19.48 ± 0.1	67.98 ± 0.1	87.46 ± 0.30
333.15	8.53 ± 0.05	–22.19 ± 0.1	67.98 ± 0.1	90.17 ± 0.30
InPc (**3Q**)				
293.15	8.50 ± 0.05	–20.69 ± 0.1	–14.94 ± 0.1	5.75 ± 0.30
303.15	8.27 ± 0.05	–20.88 ± 0.1	–14.94 ± 0.1	5.94 ± 0.30
313.15	8.13 ± 0.05	–21.08 ± 0.1	–14.94 ± 0.1	6.14 ± 0.30
323.15	7.90 ± 0.05	–21.27 ± 0.1	–14.94 ± 0.1	6.33 ± 0.30
333.15	7.76 ± 0.05	–21.47 ± 0.1	–14.94 ± 0.1	6.53 ± 0.30

(mixing of hydrophobic molecules and water) because the change in entropy (ΔS°) is large. Ross et al. suggested that, when $\Delta H^\circ < 0$, $\Delta S^\circ > 0$, the most influential force is electrostatic, when $\Delta H^\circ < 0$, $\Delta S^\circ < 0$, the most influential force is van der Waals or hydrogen bonding, and when $\Delta H^\circ > 0$, $\Delta S^\circ > 0$, the effective force is hydrophobic.[55,56] According to Table 2, it is implied that the binding process is endothermically disfavored ($\Delta H^\circ > 0$) and entropically favored ($\Delta S^\circ > 0$) for **1Q** and **2Q** while enthalpically favored ($\Delta H^\circ < 0$) process was prevailing for **3Q**.

Ross et al. reported the thermodynamic parameters associated with various kinds of interactions that may take place in protein association processes and proved that the contributions to positive entropy and enthalpy changes arose from both ionic and hydrophobic interactions.[47] Based on this literature, in the present study, stable **1Q** and/or **2Q**-DNA complexes started to form via the neutralization of cationic Pcs with phosphates of DNA. In aqueous solvent the closer proximity of **1Q** and **2Q** molecules to the DNA helix could be assigned as hydrophobic interaction due to removal of water around Pc–DNA complexes, resulting in a large increase in entropy. The neutral Pc–DNA complexes will have less electronic repulsions and interact with each other more easily. As a consequence, starting with ionic attractions between cationic small morpholinoethoxy groups and negative phosphates, the association of nonpolar parts of **1Q** and/or **2Q**-DNA complexes in a polar environment required the removal of a large amount of ordered water, causing a detrimental rise in entropy. The coordinations of zinc-N/O donors in DNA with **2Q** were the additional factor increasing entropy.

The data presented in Table 2 indicated that the favorable free energy changes of the binding process for **3Q** arose from the large negative enthalpy changes. Thus this binding process was enthalpy driven rather than entropy driven.[55] The binding process was exothermic and electrostatic according to decreasing K_{eq} values with increasing temperatures.[56] Indium–DNA coordination and axially bound chlorine resulted in the order of **3Q** molecules around DNA. As known, ordered structures require negative enthalpy while positive enthalpy shows the free motion of molecules in solvent. These calculations were in accordance with UV-Vis and the fluorescence spectra of **3Q** supported the increase in emission after putative additions of DNA.

3. Experimental

3.1. Materials and equipment

Disodium salt of deoxyribonucleic acid from calf thymus (DNA) was purchased from MP Biomedicals. Buffer solution (disodium hydrogen phosphate/ potassium dihydrogen phosphate, pH 7) was purchased from Merck. 4-(2-Hydroxyethyl)morpholine (2-morpholinoethanol) and 3-nitrophthalonitrile were purchased from Aldrich. 1,8(11), 15(18),22(25)-Tetrakis-(2-morpholinoethoxy)phthalocyanine(**1**), 1,8(11),15(18),22(25)-tetrakis-(2- morpholinoethoxy)phthalocyaninatozinc (II) (**2**), and 1,8(11), 15(18),22(25)-tetrakis-(2-morpholinoethoxy)phthalacyaninato(chloro)indium(III) (**3**) were prepared according to the literature.[57]

All reported ^{1}H NMR spectra were recorded on an Agilent VNMRS 500 MHz spectrometer. FTIR spectra were recorded on a PerkinElmer One FT-IR spectrometer and absorption spectra were recorded using Scinco LabProPlus UV/Vis spectrophotometer with 1-cm path length quartz cuvettes within the spectroscopic range of 300–800 nm. Fluorescence spectra were recorded on a PerkinElmer LS55 fluorescence spectrophotometer.

3.2. Synthesis

3.2.1. 1,8(11),15(18),22(25)-Tetrakis-(N-methyl-2-morpholinoethoxy)phthalocyanine tetraiodide (1Q)

Compound **1** (0.1 g, 0.09 mmol) was dissolved in 10 mL of chloroform and methyl iodide (0.03 mL, 0.48 mmol) in excess was added to this solution and the reaction mixture was stirred under reflux for 4 h. After cooling to room temperature the resulting suspension was filtered off, washed successively with hot ethanol, ethyl acetate, THF, chloroform, n-hexane, and diethyl ether, and dried under vacuum at 120 °C for 24 h. Yield: 0.14 g (75%). Mp > 200 °C; IR υ_{max}/cm^{-1}: 3283 (N–H), 3007 (Ar–H), 2944–2869 (Aliph–CH), 1586, 1469, 1334, 1265, 1235, 1124, 1093; UV-Vis (DMF) λ_{max}/nm: 318 (4.68), 697 (5.02), 724 (4.93); ^{1}H NMR (500 MHz,

DMSO-d_6) δ, ppm: 9.22–9.18 (m, 4H, Ar–H), 8.38–8.34 (m, 4H, Ar–H), 8.10–8.09 (d, 2H, Ar–H), 8.06–8.04 (d, 2H, Ar–H), 5.45 (br s, 4H, O–CH_2), 5.35 (br s, 4H, O–CH_2), 4.61 (br s, 4H, N–CH_2), 4.24 (br s, 4H, N–CH_2), 4.12–4.00 (m, 16H, O–CH_2), 3.86–3.73 (m, 16H, N–CH_2) 3.67 (s, 12H, CH_3), –0.13 (br s, 2H, NH); anal. calc. for $C_{60}H_{74}I_4N_{12}O_8$ (1598.95): C 45.07, H 4.65, N, 10.51; found: C 44.12, H 3.89 N 10.00; MS (MALDI-TOF): m/z 574.2 [M-4I-4R]$^+$ (R was given in Scheme).

3.2.2. 1,8(11),15(18),22(25)-Tetrakis-(N-methyl-2-morpholinoethoxy) phthalocyaninatozinc(II) tetraiodide (2Q)[58]

Compound **2** (0.1 g, 0.09 mmol) and excess of methyl iodide (0.03 mL, 0.48 mmol) in 10 mL of chloroform were heated to reflux temperature for 4 h. After cooling to room temperature the green precipitate was filtered off and washed with hot ethanol, ethyl acetate, THF, chloroform, hexane, and diethyl ether. The product was dried under vacuum at 120 °C for 24 h. Yield: 0.12 g (90%). Mp > 200 °C; IR υ_{max} /cm^{-1}: 3014 (Ar–H), 2947–2873 (Aliph–CH), 1584, 1484, 1332, 1263, 1228, 1120, 1080; UV-Vis (DMF) λ_{max}/nm: 325 (4.45), 698 (5.24); ^{1}H NMR (500 MHz, DMSO-d_6) δ, ppm: 9.19–9.14 (m, 4H, Ar–H), 8.30–8.25 (m, 4H, Ar–H), 8.04–8.02 (d, 2H, Ar–H), 7.98–7.97(d, 2H, Ar–H), 5.50 (br s, 4H, O–CH_2), 5.37 (br s, 4H, O–CH_2), 4.61 (br s, 4H, N–CH_2), 4.24 (br s, 4H, N–CH_2), 4.17–4.13 (m, 4H, O–CH_2), 4.06–4.00 (m, 12H, O–CH_2), 3.88–3.81 (m, 8H, N–CH_2), 3.70 (s, 12H, CH_3), 3.64–3.61 (m, 8H, N–CH_2); anal. calc. for $C_{60}H_{72}I_4N_{12}O_8Zn$ (1662.31): C 43.35, H 4.37, N 10.11; found: C 42.09, H 4.13, N 9.72; MS (MALDI-TOF): m/z 1390.3 [M–2I–CH_3–H]$^+$, [1248.2–3I–2CH_3–H]$^+$, 1108.8 [M–4I–3CH_3+H]$^+$.

3.2.3. 1,8(11),15(18),22(25)-Tetrakis-(N-methyl-2-morpholinoethoxy) phthalocyaninato(chloro)-indium(III) tetraiodide (3Q)

Compound **3** (0.1 g, 0.08 mmol) and excess of methyl iodide (0.03 mL, 0.48 mmol) in 10 mL of chloroform were heated to reflux temperature for 4 h. After cooling to room temperature the precipitate was filtered off and washed with hot ethanol, ethyl acetate, THF, chloroform, n-hexane, and diethyl ether. The green product was dried under vacuum at 120 °C for 24 h. Yield: 0.12 g (86%). Mp > 200 °C; IR υ_{max} /cm^{-1}: 3018 (Ar–H), 2947–2873 (Aliph–CH), 1584, 1463, 1330, 1267, 1232, 1122, 1059; UV-Vis (DMF) λ_{max}/nm: 325 (4.37), 717 (4.76); ^{1}H NMR (500 MHz, DMSO-d_6) δ, ppm: 9.19–9.16 (m, 4H, Ar–H), 8.32–8.31 (m, 4H, Ar–H), 8.07–8.00 (m, 4H, Ar–H), 5.50 (br s, 4H, O–CH_2), 5.36 (br s, 4H, O–CH_2), 4.71–4.69 (t, 4H, N–CH_2), 4.60 (br s, 4H, N–CH_2), 4.04–3.99 (m, 16H, O–CH_2), 3.68 (s, 12H, CH_3), 3.61–3.56 (m, 16H, N–CH_2); anal. calc. for $C_{60}H_{72}ClI_4InN_{12}O_8$ (1747.20): C 41.25, H 4.15, N 9.62; found: C 40.09, H 3.90, N 9.71; MS (MALDI-TOF): m/z 1711.6 [M–Cl]$^+$.

3.3. Determination of binding of quaternized Pcs (1Q–3Q) to DNA using UV-Vis titrations

All titrations of Pcs with CT-DNA were performed at room temperature in buffer solution. The concentrations of CT-DNA per nucleotide phosphate were calculated from the absorbance at 260 nm using εDNA = 13,200 M^{-1} cm^{-1}.[59] DNA was stored at 4 °C overnight and used within 2 days. The stock solutions of 25 μM quaternized Pcs (**1Q**–**3Q**) and 50 μM DNA were prepared in buffer solution. First the absorption spectrum of a 3 mL buffer solution of **1Q**, **2Q,** and **3Q** was recorded and then 6 × 30 μL for **1Q**, **2Q**, and **3Q** injections of DNA were added manually. Absorption spectra were collected from 500 nm to 800 nm. The titrations were

carried out until the Pcs' Q bands remained at a fixed wavelength upon successive additions of CT-DNA. To determine the binding constants $K_{b\mathbf{1Q}}$, $K_{b\mathbf{2Q}}$, and $K_{b\mathbf{3Q}}$, Eq. (1) was employed.[60]

$$[DNA]/(\varepsilon a - \varepsilon f) = [DNA]/(\varepsilon b - \varepsilon f) + 1/[Kb((\varepsilon b - \varepsilon f)], \quad (1)$$

where the apparent absorption coefficient εa, εf, and εb correspond to Aobserved/[Pc], the extinction coefficient of the free Pc, and the extinction coefficient of the Pc when fully bound to DNA, respectively. In plots of [DNA]/($\varepsilon a - \varepsilon f$) versus [DNA], K_b is given by the ratio of slope to intercept.[61] The experiments were repeated three times.

3.4. Determination of binding of quaternized Pcs (1Q–3Q) to DNA using fluorescence measurements

The binding properties of **1Q**, **2Q**, and **3Q** complexes to DNA were studied by spectrofluorometry at room temperature. A buffer solution of **1Q** (25 μM, 3.0 mL) (or **2Q**, **3Q**) was titrated by consecutive additions of 30-μL aliquots of 50 μM DNA. The fluorescence emission spectra were recorded after each addition of DNA. Fluorescence excitation and emission spectra were obtained from solutions of DNA and quaternized Pcs (**1Q**–**3Q**) were prepared in buffer solution. Excitation and emission slits were set at 10 nm bandpass at 900 V. **1Q** and **2Q** were excited at 690 nm and emission at 738 nm for **1Q** and 732 nm for **2Q** were observed. In the case of **3Q** the excitation and emission wavelengths were 700 and 743 nm (Table S1). Due to the substituted groups on nonperipheral positions, **1Q**–**3Q** have no aggregation in aqueous solutions so all fluorescence was observed in the absence of surfactant like Triton X-100.

3.5. Determination of the effect of quaternized Pcs (1Q–3Q) on the fluorescence intensity of DNA–SYBR complex

In order to determine the binding mode of **1Q**, **2Q**, and **3Q** to DNA, the decrease in emission of DNA–SYBR complex around 528 nm was monitored indicating the competitive binding of SYBR with quaternized Pcs (**1Q**–**3Q**). The concentration of the purchased SYBR Green was diluted to 1X. Each of six fluorescence cuvettes contained the solution of SYBR at a fixed concentration of 1X (700 μL) and the solution of DNA (50 μM, 1.8 mL). At a final concentration of 0, 0.59, 1.14, 1.68, 2.18, 2.68, and 3.18 μM 60-μL solutions of quaternized Pcs (**1Q**–**3Q**) were added to the solution of SYBR–DNA complex in each cuvette. The samples were excited at 358 nm and the fluorescence spectra were recorded from 390 to 650 nm consecutively at 900 V with a slit of 10 nm for both excitation and emission. All solutions were prepared in buffer solution.

3.6. Determination of the change in thermal denaturation profile of DNA

Melting temperatures were determined for CT-DNA (50 μM, 2.5 mL) and quaternized Pcs (**1Q**–**3Q**) (25 μM, 0.3 mL) in buffer by heating from 20 to 90 °C at a rate of 0.6 °C/min, and recording the UV absorbance at 260 nm every 10 s. The absorbance measurements were repeated five times and standard deviations were included.

3.7. Determination of thermodynamic parameters

The equilibrium constants of DNA (50 μM, 1.5 mL)–Pc (25 μM, 1.5 mL) complexes were determined by analyzing the absorbance of Pc–DNA solutions at varying temperatures (293.15 K, 303.15 K, 313.15 K, 323.15

K, 333.15 K). For the reversible binding reaction of a ligand that is binding to a DNA molecule with a single site to form a ligand–DNA complex, we can write the binding reaction as shown in Eq. (2).[62]

$$L + DNA \leftrightarrow LDNAK = [LDNA]eq/([L]eq \times [DNA]eq), \tag{2}$$

where [L] is the concentration of the ligand or DNA-binding domain (in the present work, L represents **1Q**, **2Q**, or **3Q**), and [DNA]eq and [LDNA]eq are the concentrations of DNA and bound complex at equilibrium, respectively. The stability of the bound complex is determined by the differences in the noncovalent interactions between the Pc and the DNA as temperatures varied by nonlinear least-squares algorithm.[63] At these temperatures, DNA does not undergo any structural degradation. The absorption spectra were analyzed by assuming Pc:DNA molar ratios as 1:1 and 2:1. The results show that the best fitting corresponds to the 1:1 model complex at the studied temperatures.

The energetics of DNA–Pc equilibrium can be conveniently characterized by three thermodynamic parameters, i.e. standard Gibbs free energy, ΔG°; the standard molar enthalpy, ΔH°; and the standard molar entropy, ΔS°. ΔG° can be calculated from the equilibrium constant, K, using the familiar relationship, $\Delta G^\circ = -RT\ \ln K$, in which R and T refer to the gas constant and the absolute temperature, respectively.[61]

The Van't Hoff equation gives a linear plot of lnK versus 1/T, if the heat capacity change for the reaction is essentially zero (Eq. (3)).

$$d \ln K/d(1/T) = -\Delta H^\circ/R \tag{3}$$

ΔH° can be calculated from the slope of the straight line, $-\Delta H^\circ/R$, and the standard entropy by Eq. (4).

$$\Delta S^\circ = (\Delta H^\circ - \Delta G^\circ)/T \tag{4}$$

4. Conclusion

The aim of the present work was to gain a deeper insight into the mechanism of binding processes of cationic Pcs (**1Q**–**3Q**) that are nonperipherally substituted with morpholinoethoxy moieties to DNA.

Based on the data given in Tables 1 and 2, **1Q**–**3Q** react with DNA spontaneously with high affinity. Both intra- and intermolecular forces that dominate the binding process could be the following:

a) The self-association of (especially seen in **1Q**) Pcs leads to stacking of them around DNA. Although monomeric structures were present in the aqueous media, π–π overlap between Pc molecules forces them to move in aggregates. In the case of **2Q** and **3Q**, a possible coordination of zinc or indium with any donors in DNA proved that monomers are also present in the solution. In compound **3Q**, chlorine is the most important factor to reduce aggregation, preventing π–π stacking. These are intermolecular forces among Pc molecules that are known mostly in aqueous solutions. The self-association of the compounds (**1Q**–**3Q**) is disrupted by the addition of DNA that acts as surfactant and increases the tendency towards monomers. Moreover, while the hydrophobic Pc core of **1Q**, **2Q**, and **3Q** interacts with the nonpolar interior of DNA, the attractions between cationic morpholinoethoxy groups with negative charged phosphate backbone are electrostatic.

b) The electrostatic attraction could be observed with UV-Vis spectra. The spectra show that with the increase in interaction the absorption of **1Q**–**3Q** decreases and at a certain amount of DNA the complexation of Pc–DNA occurs.

c) As known, static quenching occurs when dyes aggregate due to hydrophobic effects. They stack together to minimize contact with water. Planar aromatic dyes such as Pcs that associate through $\pi-\pi$ interactions within themselves can enhance static quenching. In our case, the addition of DNA disrupts the aggregation among Pcs and increases the fluorescence of the compounds (**1Q**–**3Q**) in two ways: 1) removing counterions and water through the electrostatic attraction of phosphates and cationic morpholinoethoxy groups; 2) preventing the rotation of Pc molecules around DNA with the coordination of Zn in **2Q** and indium in **3Q** with N/O bases of DNA.

d) Neutralization of the negative charge of phosphates with cationic morpholinoethoxy units, repulsions decrease, and DNA becomes more compact. Thus, there is a "smaller room" for existing compounds such as SYBR. After the addition of **1Q**–**3Q** to the solution of SYBR–DNA, the exclusion of SYBR leads to an increase in emission of SYBR and shows the complexation of Pc–DNA.

e) Thermodynamic data indicated that the binding process of **1Q** and **2Q** progresses with entropy-driving forces, while enthalpy dominates the mechanism for **3Q**. According to the literature, both ionic and hydrophobic interactions take place in the interaction of Pc–DNA.[55,56,64,65] Electrostatic attraction initiates the closer proximity of DNA and **1Q**, **2Q**, and **3Q** molecules and then leads to interaction of Pc core with hydrophobic parts of DNA. The decrease in Tm value of **2Q** is an indicator of Zn–DNA coordination, which destabilizes DNA.

Under the consideration of the fact that Pcs have a large and planar carbon skeleton, it is logical to interpret that the complexation of DNA–**1Q**, **2Q,** and **3Q** compounds starts with electrostatic attraction forces, which leads to a closer proximity of DNA–Pcs provided with hydrophobic interactions as well. With the assumption of the electronic attraction set between phosphates of DNA and morpholinoethoxy groups of cationic Pcs (**1Q**–**3Q**) whose planes are perpendicular to the DNA helix, grooves become the most possible and suitable pockets for binding. The increases in emissions of Pc–DNA complexes also can recall a partial intercalation of compounds (**1Q**–**3Q**) with DNA due to more rigid structures. However, at this level of knowledge, it is difficult to assign the exact mode of interaction in grooves, because several possibilities exist. Additional studies are necessary to elucidate all the factors that are responsible for the binding mechanism. Based on the thermodynamic and spectroscopic data in our work, it can be concluded that **1Q**, **2Q**, and **3Q** molecules bound to DNA spontaneously with respect to negative Gibbs energies nonspecifically. While the present study highlighted the binding of freshly synthesized, cationic, water soluble compounds (**1Q**–**3Q**) with DNA, the ongoing work on PDT is noteworthy.

Acknowledgment

This work was supported by the Scientific and Technological Research Council of Turkey (TÜBİTAK, Project no: 115Z063).

References

1. Kaliya, O. L.; Lukyanets, E. A.; Vorozhtsov, G. N. *J. Porphyr. Phthalocya.* **1999**, *3*, 592-610.
2. Fiel, R. J.; Jenkins, B. G.; Alderfer, J. L. *Cationic porphyrins - DNA complexes: specificity of binding modes,* in 23rd Jerusalem Symposium in Quantum Chemistry and Biochemistry; Pullman B, Jortner J, editors. Kluwer Academic Press: Netherlands, 1990.

3. Fiel, R. J.; Howard, J. C.; Mark, E. H.; Datta-Gupta, N. *Nucleic Acids Res.* **1979**, *6*, 3093-3118.
4. Banville, D. S.; Marzill, L. G.; Wilson, W. D. *Biochem. Biophys. Res. Commun.* **1983**, *113*, 148-154.
5. Leznoff, C. C.; Lever, A. B. P. *Phthalocyanines: Properties and Applications vols. 1–4*; VCH: New York, NY, USA, 1989–1996.
6. McKeown, N. B. *Phthalocyanine Materials Synthesis, Structure and Function*; Cambridge University Press: Cambridge, UK, 1998.
7. Kadish, K.; Smith, K. M.; Guilard, R. *The Porphyrin Handbook vols. 15–20*; Academic Press: Boston, MA, USA, 2003.
8. Calvete, M. J. F.; Dini, D.; Flom, S. R.; Hanack, M.; Pong, R. G. S.; Shirk, J. S. *Eur. J. Org. Chem.* **2005**, *16*, 3499-3509.
9. Cid, J. J.; Yum, J. H.; Jang, S. R.; Nazeeruddin, M. K.; Martinez-Ferrero, E.; Palomares, E.; Ko, J.; Gratzel, M.; Torres, T. *Angew. Chem. Int. Edit.* **2007**, *46*, 8358-8362.
10. Xiong, X. Q. Z. B.; Zhou, X.; Cao, X. P.; Zhou, Y. *Chem. Biodivers.* **2007**, *4*, 215-223.
11. Özçeşmeci, M.; Ecevit, Ö. B.; Sürgün, S.; Hamuryudan, E. *Dyes Pigments* **2013**, *96*, 52-58.
12. Kurt, Ö.; Özçeşmeci, İ.; Sesalan, B. Ş.; Koçak, M. B. *New J. Chem.* **2015**, *39*, 5767-5775.
13. Karaoğlu, H. R. P.; Gül, A.; Koçak, M. B. *Dyes Pigments* **2008**, *76*, 231-235.
14. Dumoulin, F.; Durmus, M.; Ahsen, V.; Nyokong, T. *Coord. Chem. Rev.* **2010**, *254*, 2792-2847.
15. Makhseed, S.; Machacek, M.; Alfadly, W.; Tuhl, A.; Vinodh, M.; Simunek, T.; Novakova, V.; Kubat, P.; Rudolf, E.; Zimcik, P. *Chem. Commun.* **2013**, *49*, 11149.
16. Machacek, M.; Cidlina, A.; Novakova, V.; Svec, J.; Rudolf, E.; Miletin, M.; Kucera, R.; Simunek, T.; Zimcik, P. *J. Med. Chem.* **2015**, *58*, 1736-1749.
17. Lebedeva, N. S. *Russ. Chem. Bull.* **2004**, *53*, 2674-2683.
18. Nyokong, T. *Coord. Chem. Rev.* **2007**, *251*, 1707-1722.
19. Kobayashi, N.; Fukuda, T.; Ueno, K.; Ogino, H. *J. Am. Chem. Soc.* **2001**, *123*, 10740-10741.
20. Lan, W. L.; Liu, F. R.; Ke, M. R.; Lo, P. C.; Fong, W. P.; Ng, D. K. P.; Huang, J. D. *Dyes Pigments* **2016**, *128*, 215-225.
21. Ke, M. R.; Huang, J. D.; Weng, S. M. *J Photoch. Photobio. A: Chemistry* **2009**, *201*, 23-31.
22. Kuznetsova, A. A.; Lukyanets, E. A.; Solovyeva, L. I.; Knorre, D. G.; Fedorova, O. S. *J. Biomol. Struct. Dyn.* **2008**, *26*, 307-319.
23. Çakır, V.; Çakır, D.; Göksel, M.; Durmuş, M.; Bıyıklıoğlu, Z.; Kantekin, H. *J.Photoch. Photobio. A: Chemistry* **2015**, *299*, 138-151.
24. Carvlin, M. J.; Dattagupta, N.; Fiel, R. J. *Biochem. Biophys. Res. Commun.* **1982**, *108*, 66-73.
25. Burat, A. K.; Koca, A.; Lewtak, J. P.; Gryko, D. T. *J. Porphyr. Phthalocyanines.* **2010**, *14*, 605-614.
26. Pradeep, K. M.; Venugopala, Reddy K. R. ; Harish, M. N. K.; Chidananda, B.; Ganesh, S. D.; Harish, G. S.; Ashwath, N. *Int. J. Chem. Analyt. Sci.* **2012**, *3*, 1309-1312.
27. Zheng, B. Y.; Zhang, H. P.; Ke, M. R.; Huang, J. D. *Dyes Pigments* **2013**, *99*, 185-191.
28. Doan, P.; Karjalainen, A.; Chandrasselan, J. G.; Sandberg, O.; Yli-Harja, O.; Rosholm, T.; Franzen, R.; Candeias, N. R.; Kandhavelu, M. *Eur. J. Med. Chem.* **2016**, *120*, 296-303.
29. Ladopoulou, E. M.; Matralis, A. N.; Nikitakis, A.; Kourounakis, A. P. *Bioorg. Med. Chem.* **2015**, *23*, 7015-7023.
30. Daly, S. M.; Sturge, C. R.; Greenberg, D. E. *Methods. Mol. Biol.* **2017**, *1565*, 115-122.
31. Sully, E. K.; Geller, B. L.; Li, L.; Moody, C. M.; Bailey, S. M.; Moore, A. L.; Wong, M.; Nordmann, P.; Daly, S. M.; Sturge, C. R.; Greenberg, D. E. *J. Antimicrob. Chemother.* **2017**, *72*, 782-790.

32. Wesolowski, D.; Alonso, D.; Altman, S. *PNAS* **2013**, *110*, 8686-8689.
33. Evren, D.; Burat, A. K.; Özçeşmeci, İ.; Sesalan, B. Ş. *Dyes Pigments* **2013**, *96*, 475-482.
34. Öztürk, R.; Kalay, Ş.; Kalkan, A.; Türkan, A.; Abasıyanık, M. F.; Bayır, Z. A.; Gül, A. *J. Porphyr. Phthalocya.* **2008**, *12*, 932-941.
35. Yıldız, B. T.; Sezgin, T.; Çakar, Z. P.; Uslan, C.; Sesalan, B. Ş.; Gül, A. *Synthetic Met.* **2011**, *161*, 1720-1724.
36. Uslan, C.; Sesalan, B. Ş. *Dyes Pigments* **2012**, *94*, 127-135.
37. Evren, D.; Özçeşmeci, İ.; Sesalan, B. Ş.; Burat, A. K. *Synthetic Met.* **2013**, *168*, 31-35.
38. Barut, B.; Sofuoğlu, A.; Biyiklioglu, Z.; Özel, A. *Dalton. Trans.* **2016**, *45*, 14301-14310.
39. Zhu, Y. J.; Huang, J. D.; Jiang, X. J.; Sun, J. C. *Inorg. Chem. Commun.* **2006**, *9*, 473-477.
40. Kobayashi, N.; Ogata, H.; Nonaka, N., Luk'yanets, E. A. *Chem. Eur. J.* **2003**, *9*, 5123-5134.
41. Kobayashi, N.; Sasaki, N.; Higashi, Y.; Osa, T. *Inorg. Chem.* **1995**, *34*, 1636-1637.
42. Evren, D.; Yenilmez, H. Y.; Burat, A. K. *Turk. J. Chem.* **2014**, *38*, 1174-1184.
43. Poddutoori, P.; Poddutoori, P. K.; Maiya, B. G. *J. Porphyr. Phthalocya.* **2006**, *10*, 1-12.
44. Palchaudhuri, R.; Hergenrother, P. J. *Curr. Opin. Biotechnol.* **2007**, *18*, 497-503.
45. Buck-Koehntop, B. A.; Stanfield, R. L.; Ekiert, D. C.; Martinez-Yamout, M. A.; Dyson, H. J.; Wilson, I. A.; Wright, P. E. *Proc. Natl. Acad. Sci. U.S.A.* **2012**, *109*, 15229-15234.
46. Anastassopoulou, J. *J. Mol. Struct.* **2003**, *651*, 19-26.
47. Turel, I.; Kljun, J. *Curr. Top. Med. Chem.* **2011**, *11*, 2661-2687.
48. Zorlu, Y.; Kumru, U.; İşçi, Ü.; Divrik, B.; Jeanneau, E.; Albrieux, F.; Dede, Y.; Ahsen, V.; Dumoulin, F. *Chem. Commun.* **2015**, *51*, 6580.
49. Özlüer, C.; Kara, H. E. S. *J. Photoch. Photobio. B* **2014**, *138*, 36-42.
50. Byrn, S. R.; Dolch, G. D. *J. Pharm. Sci.* **1978**, *67*, 688-693.
51. Duan, W.; Wang, Z.; Cook, M. J. *J. Porphyr. Phthalocya.* **2009**, *13*, 1255-1261.
52. Bhattacharya, S.; Mandal, S. S. *Biochim. Biophys. Acta.* **1997**, *1323*, 29-44.
53. Cosa, G.; Focsaneanu, K. S.; McLean, J. R. N.; McNamee, J. P.; Scaiano, J. C. *Photoch. Photobio.* **2001**, *73*, 585-599.
54. Wartell, R. M.; Benight, A. S. *Physics Reports* **1985**, *126*, 67-107.
55. Ross, P. D.; Subramanian, S. *Biochem.* **1981**, *20*, 3096-3102.
56. Breslauer, J. K.; Remeta, D. P.; Chou, W.; Ferrante, R.; Curry, J.; Zaunczkowski, D.; Snyder, J. G.; Marky, L. A. *Biochemistry-Proc. Nati. Acad. Sci. USA* **1987**, *84*, 8922-8926.
57. Tuncer, S.; Kaya, K.; Özçeşmeci, İ.; Burat, A. K. *J. Organomet. Chem.* **2017**, *827*, 78-85.
58. Zheng, B. Y.; Ke, M. R.; Lan, W. L.; Guo, J.; Wan, D. H.; Cheong, L. Z.; Huang, J. D. *Eur. J. Med. Chem.* **2016**, *114*, 380-389.
59. Wolfe, A.; Shimer, G. H.; Meehan, T. *Biochemistry* **1987**, *26*, 6392-6396.
60. Sohrabi, N. *J. Pharm Sci. Res.* **2015**, *7*, 533-537.
61. Safaei, E.; Ranjbar, B.; Hasani, L. *J. Porphyr. Phthalocya.* **2007**, *11*, 805-814.
62. Thompson, M.; Woodbury, N. W. *Biochemistry* **2000**, *39*, 4327-4338.
63. Dezhampanah, H.; Darvishzad, T.; Aghazadeh, M. *Spectroscopy* **2011**, *26*, 357-365.
64. Privalov, P. L.; Dragan, A. I.; Crane-Robinson, C. *Nucleic Acids Res.* **2011**, *39*, 2483-2491.
65. Lebedeva, N. S.; Pavlycheva, N. A.; Parfenyuk, E. V.; Vyugin, A. I. J. *Chem. Thermodynamics* **2006**, *38*, 165-172.

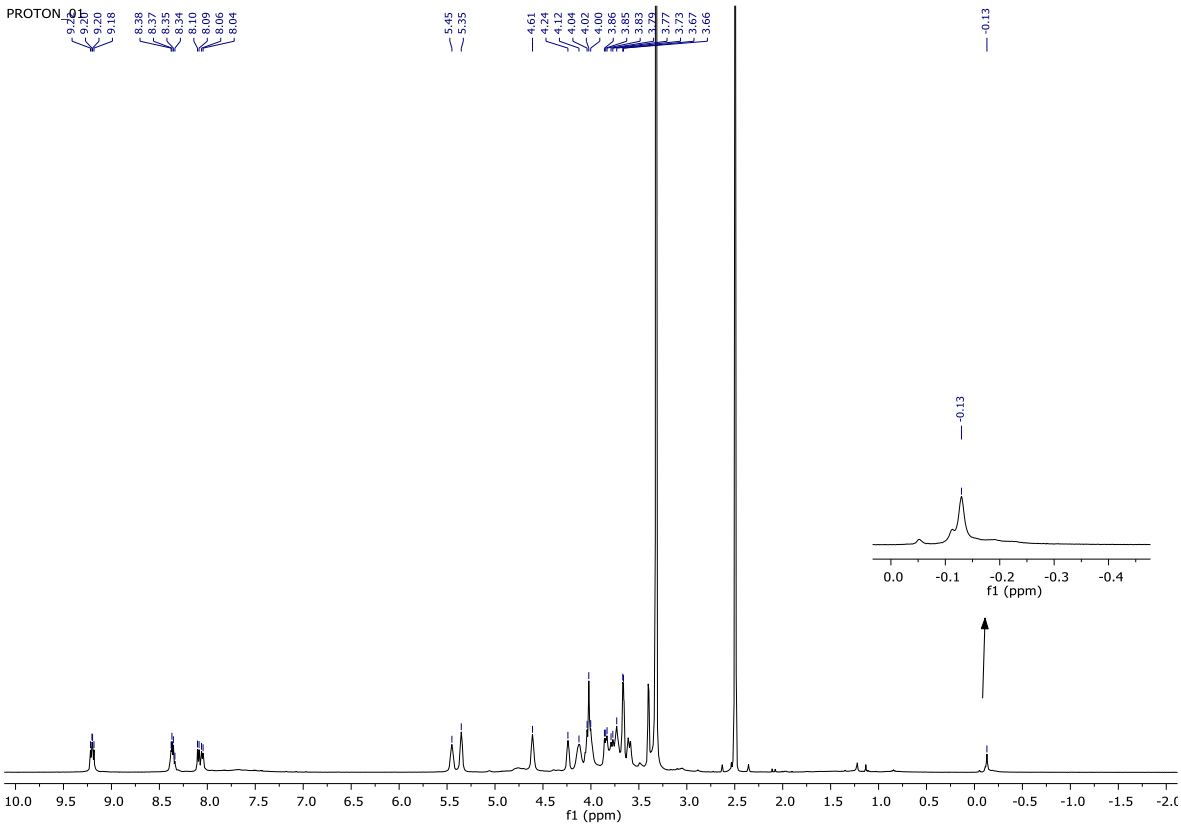

Figure S1. [1]H NMR spectrum of quaternized metal-free phthalocyanine (**1Q**) in DMSO-d_6.

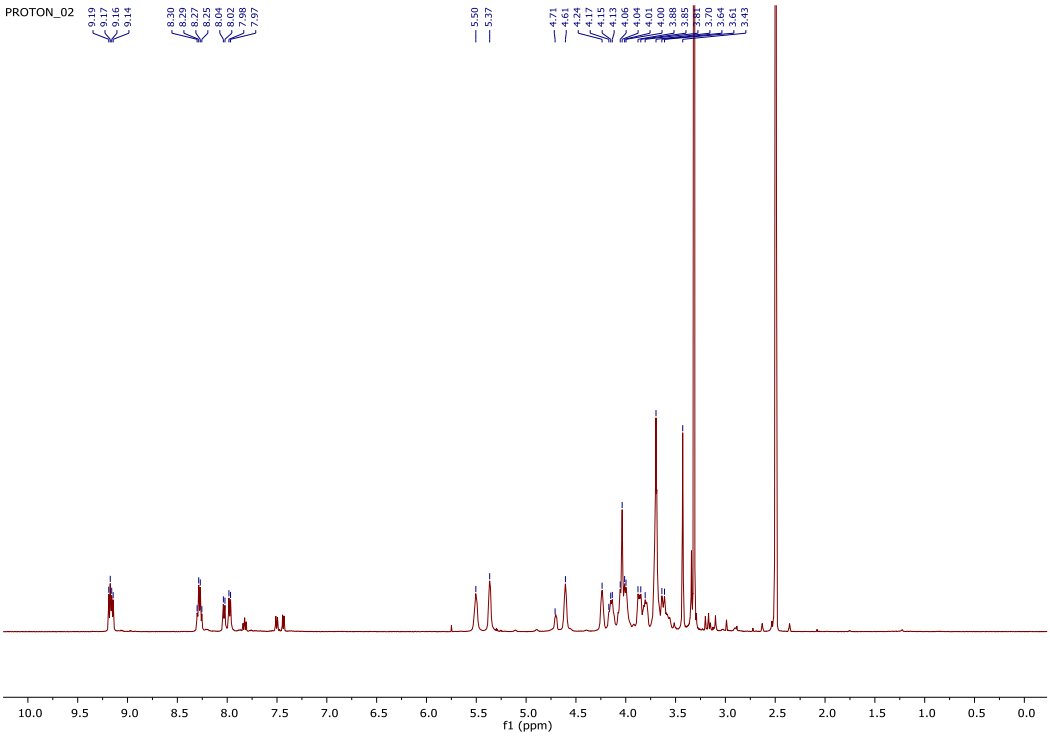

Figure S2. [1]H NMR spectrum of quaternized zinc phthalocyanine (**2Q**) in DMSO-d_6.

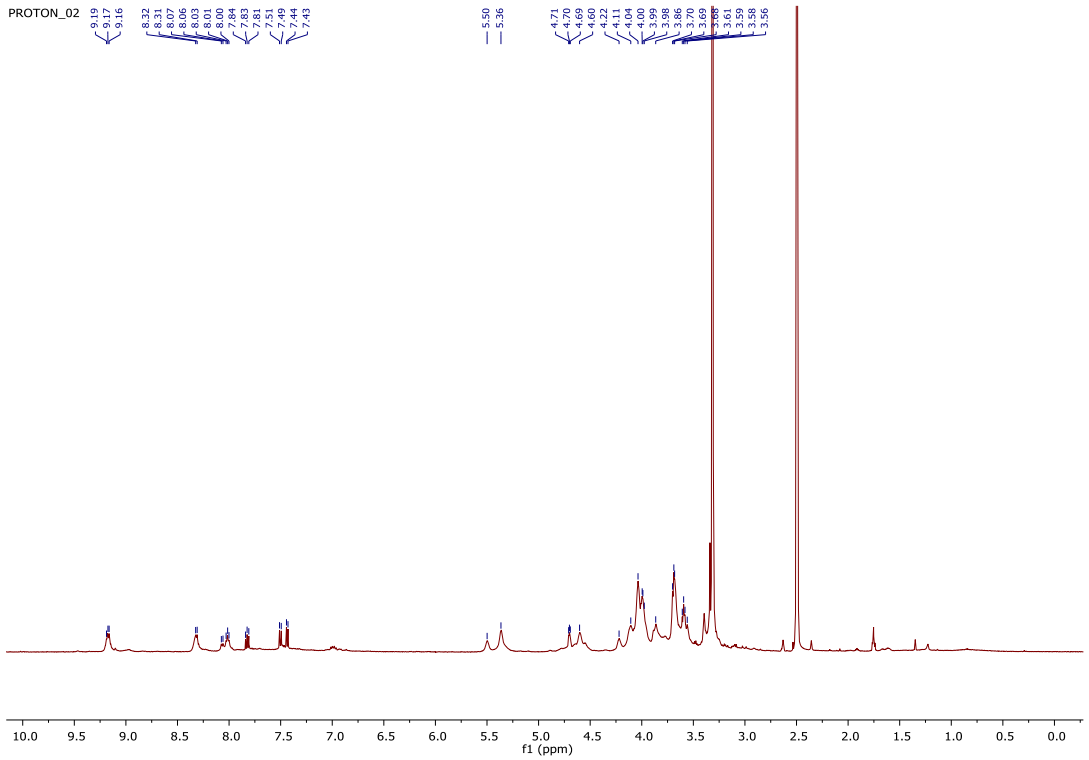

Figure S3. ^{1}H NMR spectrum of quaternized indium phthalocyanine (**3Q**) in DMSO-d_6.

Note 1: The ^{1}H NMR spectra of compounds **1Q–3Q** are somewhat broader than the corresponding signals in the starting mono substituted dinitrile derivative.[1] This broadening is likely due to chemical exchange caused by aggregation–disaggregation equilibria and the fact that the product obtained in these reactions is a mixture of positional isomers that are expected to show chemical shifts that differ slightly from each other.[2,3]

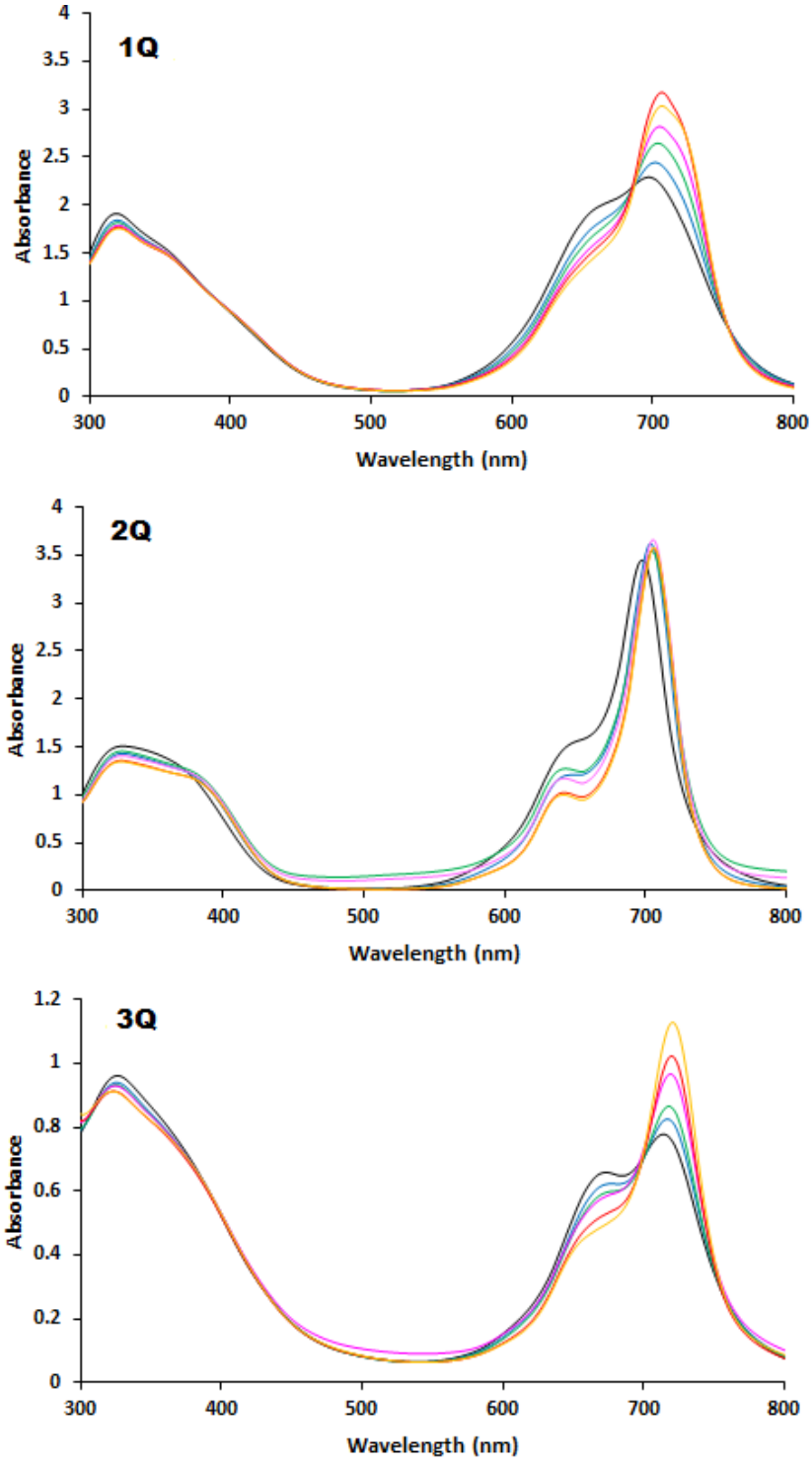

Figure S4. UV-Vis absorption spectra of quaternized metal-free (**1Q**), zinc (**2Q**), and indium (**3Q**) phthalocyanines in water (5×10^{-5} M) and water containing pyridine (60 μL–300 μL).

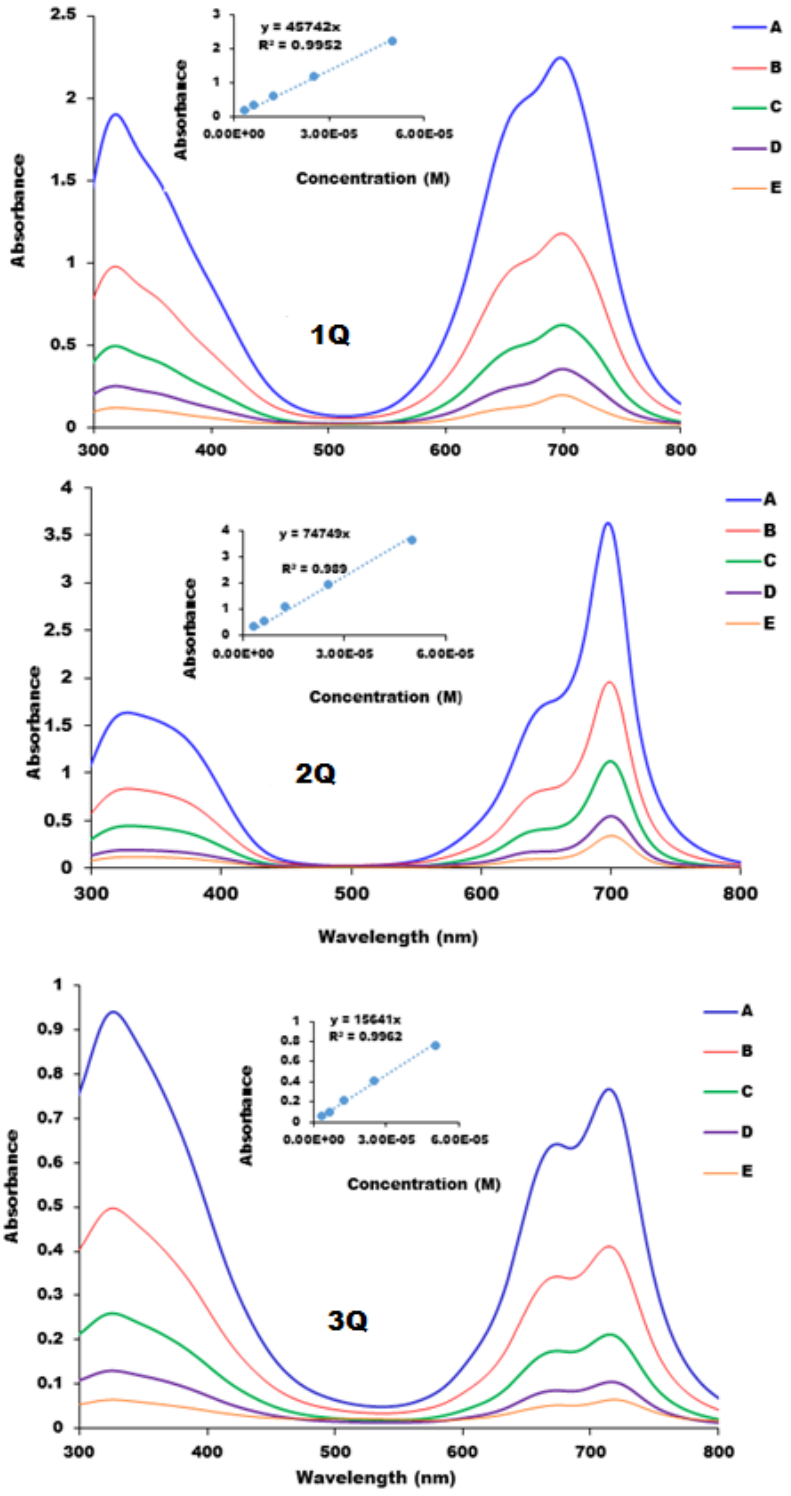

Figure S5. Aggregation behavior of quaternized metal-free (**1Q**), zinc (**2Q**), and indium (**3Q**) phthalocyanines in water at different concentrations: 5×10^{-5} M (A), 2.50×10^{-5} M (B), 1.25×10^{-5} M (C), 6.25×10^{-6} M (D), 3.125×10^{-6} M (E).

Table S1. Photophysical parameters of **1Q–3Q** in buffer solution.

	B band λ max, (nm)	log ε	Q band λ max, (nm)	log ε	Excitation λ Ex, (nm)	Emission λ Em, (nm)	Stokes shift (nm)	Φ_F
1Q	349	4.49	701	4.48	690	738	38	0.103
2Q	362	4.56	701	4.90	690	732	31	0.051
3Q	346	4.46	715	4.35	700	743	28	0.017

Note 2: Fluorescence quantum yields (Φ_F) were determined by the comparative method (Eq. (1))[4]

$$\Phi_F = \Phi_F(_{Std}) \, (FA_{Std}\eta^2 / F_{Std}A\eta^2_{Std}), \quad (1)$$

where F and F_{Std} are the areas under the fluorescence curves of phthalocyanines derivatives and the standard, respectively. A and A_{Std} are the respective absorbances of the sample and standard at the excitation and η and η_{Std} are the refractive indices of solvents used for the sample and standard, respectively. ZnPc was employed as a standard in DMF ($\Phi_F = 0.23$).[5] Both the sample and the standard were excited at the same wavelength.

References

1. Tuncer, S.; Kaya, K.; Özçeşmeci, İ.; Burat, A. K. *J. Organomet. Chem.* **2017**, *827*, 78-85.

2. Hanack, M.; Meng, D.; Beck, A.; Sommerauer, M.; Subramanian, L. R. *J. Chem. Soc. Chem. Commun.* **1993**, *1*, 58-60.

3. Gaspard, S.; Maillard, P. *Tetrahedron* **1987**, *43*, 1083-1090.

4. Ogunsipe, A.; Nyokong, T. *J. Photochem. Photobiol. A-Chem.* **2005**, *173*, 211-220.

5. Scalise, N.; Durantini, E. N. *Bioorg. Med. Chem.* **2005**, *13*, 3037-3045.